Gutzwiller approach to the Bose-Hubbard model with random local impurities

Pierfrancesco Buonsante,[1,2] Francesco Massel,[2] Vittorio Penna,[2,1] and Alessandro Vezzani[3,4]
[1]*CNISM Unità di Ricerca Politecnico di Torino, Corso Duca degli Abruzzi 24, I-10129 Torino, Italy*
[2]*Dipartimento di Fisica, Politecnico di Torino, Corso Duca degli Abruzzi 24, I-10129 Torino, Italy*
[3]*CNR-INFM, S3, National Research Center, Dipartimento di Fisica, via Campi 213/a, 41100 Modena, Italy*
[4]*Dipartimento di Fisica, Università degli Studi di Parma Viale G.P. Usberti 7/a, I-43100 Parma, Italy*
(Received 1 August 2008; published 26 January 2009)

Recently it has been suggested that fermions whose hopping amplitude is quenched to extremely low values provide a convenient source of local disorder for lattice bosonic systems realized in current experiment on ultracold atoms. Here we investigate the phase diagram of such systems, which provide the experimental realization of a Bose-Hubbard model whose local potentials are randomly extracted from a binary distribution. Adopting a site-dependent Gutzwiller description of the state of the system, we address one- and two-dimensional lattices and obtain results agreeing with previous findings, as far as the compressibility of the system is concerned. We discuss the expected peaks in the experimental excitation spectrum of the system, related to the incompressible phases, and the superfluid character of the partially compressible regions characterizing the phase diagram of systems with binary disorder. In our investigation we make use of several analytical results whose derivation is described in appendixes, and whose validity is not limited to the system under concern.

DOI: 10.1103/PhysRevA.79.013623 PACS number(s): 03.75.Lm, 03.75.Mn, 05.30.Jp, 73.43.Nq

I. INTRODUCTION

Since the seminal paper by Fisher *et al.* [1], disordered bosonic lattice systems have been the subject of active investigation. The recent impressive advances in cold atom trapping allowed the experimental realization of the prototypal bosonic lattice model, i.e., the Bose-Hubbard model [2]. Different techniques have been devised for the introduction of disorder in the system [3], such as speckle field patterns [4], incommensurate bichromatic optical lattices [5], and localized fermionic impurities [6]. In particular Ref. [5] provides experimental evidences of the hallmark phase of the disordered Bose-Hubbard model, i.e., the compressible and nonsuperfluid Bose glass [1].

At the theoretical level very diverse techniques have been employed in the study of the disordered Bose-Hubbard model. A nonexhaustive list includes field-theoretical techniques [1,7], quantum Monte Carlo simulations [8,9], mean-field schemes [10–16], and others [17–20].

Here we are interested in the case of fermionic impurities. Bose-Fermi systems have been studied by several authors [21]. If the kinetic energy of the fermionic atoms is negligible, e.g., due to a strong suppression of the relevant hopping amplitude, the impurities localize at random sites of the optical lattice [6,22,23]. The system can be hence described by a Bose-Hubbard model with random local potential characterized by a binary distribution. An early partial discussion of the phase diagram of this model [24] has been recently complemented by several authors [23,25–27]. A characteristic feature evidenced by these works consists in the presence of incompressible phases corresponding to noninteger fillings. Mering and Fleischhauer [23] provide simple arguments showing that the phase diagram of the 1D disordered model does not depend on the impurity density and can be straightforwardly derived by that of the homogeneous case, at least as far as compressibility is concerned. In particular one can recognize fully compressible, fully incompressible, and partially compressible regions. While the first and the second are clearly superfluid and insulating, respectively, the question arises about the superfluidity of the partially compressible regions, at least on high dimensional lattices. Indeed, as discussed in Refs. [23,26], the partially compressible phase is bound to be insulating, and hence Bose glass, on 1D lattices.

In this paper we describe the zero-temperature mean-field phase diagram of the Bose-Hubbard model with binary-distributed disorder. First of all, we show that the above compressibility scenario independent of the impurity density [23] is also confirmed by our site-dependent Gutzwiller approach. Moreover, the analytical tractability and the computational affordability of this technique allows us to investigate the superfluidity of the partially compressible phase both in one and two dimensional systems. In particular, we address the issue of quantum percolation which, as already pointed out in Ref. [6], is expected to play a crucial role in this problem. While we confirm that on one-dimensional systems the partially compressible phase is substantially insulating, we find that in higher dimensions the system always exhibits a finite superfluid fraction due to quantum tunneling. However, this superfluid fraction can be so small that the system can be considered virtually insulating. Although phase diagrams make rigorous sense in the thermodynamic limit, it should be taken into account that the linear dimension of current experimental realizations of the system under concern is of the order of a few hundred sites. It is hence important to consider finite-size effects, which we demonstrate to be quite relevant especially in the partially compressible phases, and to depend significantly on the impurity density.

The plan of the paper is as follows. In Sec. II we describe the model under investigation and introduce the superfluid fraction as an important parameter in the characterization of the phase diagram thereby. In Sec. III we recall the site-

dependent Gutzwiller approach and provide analytic expressions for the superfluid fraction and the flux induced by an infinitesimal velocity field in this framework. Section IV is devoted to the phase diagram of the system. First of all we discuss how the compressibility scenario argued in Ref. [23] is captured by the site-dependent mean-field approach. In Sec. IV A we provide an analytical form for the boundaries of the fully incompressible insulating lobes. Moreover, we discuss how the excitation spectrum of the system [5] is modified by the presence of the noninteger insulating phases characterizing the Bose-Hubbard model with binary disorder. Section IV B discusses the superfluidity of the partially compressible phase, in relation to the quantum percolation phenomenon. Finally, finite-size effects are investigated in Sec. IV C for 1D and 2D systems. This paper also contains appendixes where several interesting analytical results are provided for the site-dependent Gutzwiller approach. In particular in Appendix A we clarify the connection between the mean-field Hamiltonian and the dynamical Gutzwiller equations. In Appendix B the analytic formula for the boundaries of the incompressible lobes is derived explicitly. Also, we provide an useful inequality and clarify the connection between such a formula and similar results derived in effective single site mean-field approaches [1,12,16,19,25]. Finally, the superfluid fraction and the flux across neighboring sites is derived analytically as a function of the mean-field order parameters alone in Appendix C. A particularly simple expression applying in the 1D case is also provided. We emphasize that the results discussed in the appendices are not limited to the case of binary distributed disorder considered in Secs. II–V.

II. THE MODEL

The system under investigation is described by the Bose-Hubbard Hamiltonian

$$H = \frac{U}{2}\sum_{j=1}^{M} n_j(n_j-1) + \sum_{j}^{M} v_j n_j - t\sum_{i,j} A_{i,j} a_i^\dagger a_j. \tag{1}$$

The on-site bosonic operators a_j, $a_j^\dagger$ and $n_j=a_j^\dagger a_j$ destroy, create, and count particles at lattice site j, respectively. The geometry of the M-site lattice is described by the adjacency matrix A, whose generic element A_{ij} equals 1 if sites i and j are nearest neighbors, and 0 otherwise. The parameters U and t are the on-site repulsive strength and the hopping amplitude across neighboring sites and, from the experimental point of view, they are related to the scattering length of the alkali-metal atoms forming the bosonic gas and the strength of the optical lattice [28]. We will be considering a binary random distribution for the local potential v_j [29], namely,

$$p(v_j) = p_0\delta(v_j-\Delta) + (1-p_0)\delta(v_j). \tag{2}$$

This choice is meant to account for the presence of $N_{\mathrm{imp}}=Mp_0$ atoms of a second species trapped at randomly determined sites by a strong quench in the relevant hopping amplitude [6,22,23,30]. This requires that the hopping amplitude of the bosonic species described by Hamiltonian (1) and that of the species acting as a source of localized impurities can be controlled independently [22,23,25,26,30]. In particular, the latter can be made virtually zero in order to ensure that the impurities stay localized while the bosons can attain their ground state configuration. The parameter Δ measures the strength of the interaction between these frozen impurities and the bosons described by Hamiltonian (1). In most of the following discussion we assume $\Delta < U$. The general case can be worked out straightforwardly, and it is briefly discussed in Sec. IV A.

As is well known [1], on a homogeneous lattice $v_j=0$, the zero-temperature phase diagram of the Bose-Hubbard model described by Eq. (1) comprises an extended superfluid (SF) region and a series of Mott-insulator (MI) lobes. The SF phase is gapless, compressible, and characterized by nonvanishing superfluid fraction. Conversely, the MI phase is gapped, incompressible, and characterized by vanishing superfluid and condensate fractions. The presence of random potentials is expected to induce a further Bose-glass (BG) phase which, similar to MI is not superfluid, but, similar to SF, is gapless and compressible [1]. Recently, it has been shown that in the case of uniformly box-distributed disorder such a phase can be captured by a multiple-site mean-field approach [13–15], both on one- [13,14] and two-dimensional lattices [15]. In the latter case the presence of the harmonic trapping potential typical of experimental systems was also taken into account.

The superfluid fraction is estimated as the response of the system to an the infinitesimal velocity field imposed on the lattice. In the general case such a field is described by the antisymmetric matrix $B_{ij}=-B_{ji}$ having nonzero elements only across neighboring sites. In the reference frame of the moving lattice the Hamiltonian of the system has the same form as Eq. (1) except that A_{ij} is substituted by $A_{ij}\exp(i\theta B_{ij})$, where θ is a scalar related to the modulus of the velocity field (see, e.g., Refs. [31,32]). The superfluid fraction is often defined as the stiffness of the system under the phase variation imposed by the velocity field (see, e.g., Refs. [33–35])

$$f_{\mathrm{s}} = \lim_{\theta\to 0} \frac{E_\theta - E_0}{tN\theta^2}, \tag{3}$$

where E_θ and E_0 are the ground-state energies of the system when the lattice is moving and at rest, respectively, while N is the total number of bosons in the system. It should be noticed that Eq. (3) is properly a fraction, i.e., a quantity with values in the interval [0, 1], only in simple situations, such as a homogeneous velocity field. More in general, the condition $\max(|B_{ij}|)\leqslant 1$ ensures that the superfluid fraction does not exceed 1. The imposition of a velocity field induces a flux across neighboring sites i and j of the form

$$\mathcal{J}_{ij} = itA_{ij}\langle\Psi|e^{-i\theta B_{ij}}a_j^\dagger a_i - e^{i\theta B_{ij}}a_i^\dagger a_j|\Psi\rangle, \tag{4}$$

which clearly vanishes for $\theta=0$. In the following we will show that $f_{\mathrm{s}}=0$ only if $\mathcal{J}_{ij}=0$ for any pair of neighboring sites.

III. MEAN-FIELD APPROXIMATION

The results we are going to illustrate are obtained in the widely used site-decoupling mean-field approximation [36,37]. Despite this approach cannot capture the correct behavior of the spatial quantum correlations, it provides a qualitatively satisfactory picture of the phases of strongly correlated systems, even in the presence of spatial inhomogeneities arising from the harmonic confinement typical of experiments [38] or from superimposed disordered potentials [10,13,15].

In the strongly correlated regime the state of the system is expected to be well approximated by a Gutzwiller product state

$$|\Psi\rangle = \bigotimes_j |\psi_j\rangle, \quad |\psi_j\rangle = \sum_{\nu=0}^{\infty} c_{j\nu} \frac{(a_j^\dagger)^\nu}{\sqrt{n!}} |\Omega\rangle, \tag{5}$$

where $|\Omega\rangle$ is the vacuum state, $a_j|\Omega\rangle = 0$. A time-dependent variational principle similar to that illustrated in Ref. [39] results in a set of nonlinear dynamical equations for the expansion coefficients $c_{j\nu}$ [40]. It can be shown that finding the minimum-energy stationary state (fixed-point) of such equations is equivalent to finding the ground state of the mean-field Hamiltonian

$$\mathcal{H} = \sum \mathcal{H}_i + t \sum_{ij} \alpha_i^* A_{i,j} \alpha_j e^{i\theta B_{i,j}}, \tag{6}$$

$$\mathcal{H}_i = \frac{U}{2} a_i^\dagger a_i^\dagger a_i a_i + (v_i - \mu) a_i^\dagger a_i - t(\gamma_i a_i^\dagger + \gamma_i^* a_i) \tag{7}$$

subject to the self-consistent condition

$$\gamma_i = \sum_j A_{i,j} \alpha_j e^{i\theta B_{i,j}}, \quad \alpha_i = \langle \Psi | a_i | \Psi \rangle = \langle \psi_i | a_i | \psi_i \rangle. \tag{8}$$

Such a mean-field Hamiltonian is usually derived by introducing the decoupling assumption $a_i^\dagger a_j \approx a_i^\dagger \alpha_j + \alpha_i^* a_j - \alpha_i^* \alpha_j$ in Hamiltonian (1) [37]. These issues will be briefly discussed in Appendix A. The parameter μ appearing in Eq. (7) is the so-called "chemical potential," which comes about due to the fact that the mean-field Hamiltonian (6) does not preserve the total number of bosons, unlike Eq. (1).

The mean-field order parameters α_i (with $\theta = 0$) allow the characterization of the quantum phases of the system, as far as compressibility is concerned. In particular, on a homogenous system the (site-independent) α_i is zero in the incompressible insulator and finite in compressible superfluid phase [37]. On inhomogenous lattices a further situation can in principle occur, where $\alpha_i \neq 0$ only on a fraction of the lattice sites. Following Ref. [23] we will define such a situation as partially compressible, as opposed to the fully compressible and fully incompressible phases corresponding to the MI and SF.

We observe that in this framework the one-body density matrix has a rather simple expression

$$\rho_{ij} = \frac{\langle \Psi | a_i^\dagger a_j | \Psi \rangle}{N} = \frac{\delta_{ij} \langle \psi_j | n_j | \psi_j \rangle + (1 - \delta_{ij}) \alpha_i^* \alpha_j}{N} \tag{9}$$

so that the condensate fraction, i.e., the largest eigenvalue of ρ_{ij} [41], can be estimated as

$$f_c \propto \frac{1}{N} \sum_i |\alpha_i|^2. \tag{10}$$

Such a form shows that, at the mean field level, the condensate fraction vanishes only for fully uncompressible MI phases. Actually f_c has been used as a convenient order parameter in Refs. [13–15,42].

As one expects, the presence of the velocity field involved in the evaluation of the superfluid fraction modifies the self-consistently determined mean-field parameters defined in Eq. (8). It is easy to show that in the homogeneous case the superfluid fraction defined in Eqs. (3) equals the right-hand side of Eq. (10). That is, the superfluid and condensate fractions coincide and can be equivalently employed for characterizing the phase diagram of the system. In the general case a perturbative approach, carried out in Appendix C, shows that the superfluid fraction is

$$f_s = \frac{1}{2N} \sum_{i,j} A_{ij} \alpha_i^0 \alpha_j^0 (B_{ij} - \phi_i + \phi_j)^2, \tag{11}$$

where the real and positive α_j^0 are the mean-field order parameters for $\theta = 0$, and the real phase factors ϕ_j depend on the α_j^0 according to Eq. (C7). At the first perturbative order in θ, the mean-field order parameter are

$$\alpha_j = \alpha_j^0 \exp(i\theta\phi_j), \tag{12}$$

while the flux defined in Eq. (4) becomes

$$\mathcal{J}_{ij} = 2\theta t \alpha_i^0 \alpha_j^0 A_{ij} [B_{ij} - \phi_i + \phi_j]. \tag{13}$$

Clearly, the superfluid fraction in Eq. (11) vanishes only if each of the terms in the sum vanishes, i.e., if all of the fluxes in Eq. (13) are zero. Expectedly, this happens in the MI phase, where $\alpha_j^0 = 0$ at every site. The same can happen under more general conditions. Indeed, it is sufficient that $\phi_i - \phi_j = B_{i,j}$ whenever $\alpha_i^0 \alpha_j^0 \neq 0$. This is precisely what happens in a BG phase, where $f_s = 0$ despite the system is compressible.

It is interesting to note that on 1D systems, owing to the conservation of flux, the evaluations of Eqs. (13) and (11) does not require the determination of the phases ϕ_j via Eq. (C7). Indeed, as illustrated in Appendix C, one gets

$$\mathcal{J}_{jj+1} = -\mathcal{J}_{j+1j} = \mathcal{J} = 2t\theta \left(\sum_\ell \frac{1}{\alpha_\ell^0 \alpha_{\ell+1}^0} \right)^{-1} \tag{14}$$

and

$$f_s = \frac{\mathcal{J}}{2\theta t N}. \tag{15}$$

It is clear from Eq. (14) that $\mathcal{J} = 0$ and $f_s = 0$ as soon as one of the local mean-field parameters vanishes. This explicitly shows that the partially compressible phase is insulating, and hence Bose glass, in the 1D system, as already mentioned [23,26].

IV. PHASE DIAGRAM

As discussed in Ref. [23], the zero-temperature phase diagram of the system with binary disorder can be easily inferred from that of a homogeneous system, at least as far as compressibility is concerned. Indeed, independent of the impurity density N_{imp}/M, in the thermodynamic limit $M\to\infty$ a finite fraction of the disordered system consists of arbitrarily large regions of uniform local potential (Lifschitz rare regions, see Refs. [23,26]). The bulk of these regions will behave as a homogeneous lattice, undergoing a transition at the analytically known critical value [1]

$$\frac{t}{U}=\frac{1}{2d}\mathcal{B}\left(\frac{\mu-v}{U}\right),\quad \mathcal{B}(x)=\frac{(x-\lfloor x\rfloor)(\lceil x\rceil-x)}{x+1},\qquad (16)$$

where $\lfloor x\rfloor$ denotes the largest integer smaller than x, $\lceil x\rceil=\lfloor x\rfloor+1$, d is the lattice dimension, and v is the local potential within the homogeneous regions, which can attain the values 0 and Δ. It is clear that the system is fully compressible or fully incompressible only if all of the above regions exhibit the relevant property. This means that the region of the phase diagram

$$\frac{t}{U}>\mathcal{B}_1\left(\frac{\mu}{U},\frac{\Delta}{U}\right)=\frac{1}{2d}\max\left[\mathcal{B}\left(\frac{\mu-\Delta}{U}\right),\mathcal{B}\left(\frac{\mu}{U}\right)\right]\qquad (17)$$

is fully compressible, while the incompressible lobes correspond to the region

$$\frac{t}{U}<\mathcal{B}_2\left(\frac{\mu}{U},\frac{\Delta}{U}\right)=\frac{1}{2d}\min\left[\mathcal{B}\left(\frac{\mu-\Delta}{U}\right),\mathcal{B}\left(\frac{\mu}{U}\right)\right].\qquad (18)$$

Figure 1 shows the phase diagram of the system for $\Delta=0.5U$. The fully compressible and fully incompressible regions correspond to white and dark gray shading. As in the homogeneous case, the fully incompressible lobes correspond to plateaus of the system filling. Interestingly, the binary disorder causes the appearance of non-integer critical fillings of the form $\lceil\mu/U\rceil-p_0$, where p_0 is the impurity density [23,25,26]. The incompressible MI phases will be discussed in detail in Sec. IV A. The light gray region of Fig. 1, enclosed between the boundaries $\mathcal{B}_1$ and $\mathcal{B}_2$, is of course compressible, yet it contains arbitrarily large incompressible regions. Therefore it is referred to as partially compressible [23].

This apparently simple scenario requires some clarifications when the possible superfluidity of the system is concerned. As it can be understood from Eq. (13), the system can sustain a superfluid flow only along a path where the mean field parameters α_j are not vanishing. Hence, as expected, the system is not superfluid in the incompressible regions of the phase diagram. Conversely, in the fully compressible region the mean-field parameters are nonzero almost everywhere, and a finite superfluid fraction is expected. The most interesting regions are the partially compressible ones, which can behave as BG phases, as will be discussed in Secs. IV B and IV C.

Before getting into details, it is interesting to compare the above-sketched incompressible domains with those obtained for different choices of the disordered potentials. As is well known [1], in the presence of random potentials uniformly distributed in $[-\Delta,\Delta]$ only integer-filling Mott-lobes appear, as in the homogeneous case. One of the most evident differences with respect to this case is that the bases of such lobes are not contiguous any more, being separated by Bose-glass regions of width 2Δ centered at the discrete values of the chemical potential $\mu=kU$, with $k\in\mathbb{N}$. We note that this situation is recovered by a straightforward generalization of the arguments illustrated in Appendix B. As discussed in Refs. [9,18], incompressible phases at noninteger filling—referred to as "incommensurate charge-density-wave" or "incommensurate band insulator" phases—appear also in the case of quasiperiodic random potentials. One of the main differences with respect to the present case is that the density plateaus related to the above phases disappear in the limit of vanishing hopping amplitude, reminiscent of what happens for superlattice potentials [43]. Also, the quasiperiodic nature of the local potentials rules out the Lifshitz regions which provide a profitable resource in the determination of the phase boundaries in the present case and in its generalizations [23,26]. Actually, the study of incommensurate incompressible phases in quasiperiodic random lattices appears to be a rather challenging task. For instance, the relation between the critical fillings and the incommensurability parameter of the quasiperiodic potential is well understood only in the hardcore limit, while the situation is considerably less clear in the case of softcore bosons [9,18,20]. In fact, the above-discussed phases would elude the site-decoupling mean-field approach employed here, and could be possibly captured by more refined mean-field schemes such as those described in

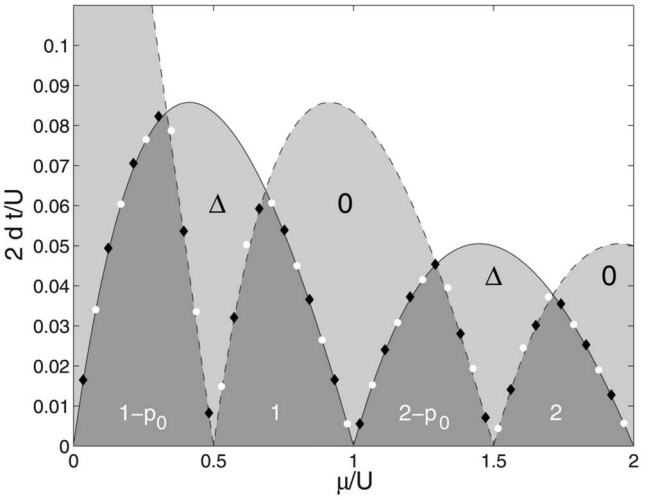

FIG. 1. Expected phase diagram for a d-dimensional lattice. The solid and dashed black curves are the (mean-field) boundaries involved in Eq. (16). These delimit three phases, as far as compressibility is concerned. The uncompressible lobes (dark gray), the partially compressible regions (light gray), and the fully compressible region (white). The uncompressible regions are labeled by the relevant filling. The partially compressible regions are labeled by the local potential of the favorable sublattice (see text for more details). The data points have been obtained as described in Sec. IV A for a very large 1D lattice ($M=10^5$) and two impurity densities $p_0=0.2$ (white circles) and $p_0=0.6$ (black circles). Note that both data sets agree very well with the expected density-independent analytic result, (18).

Ref. [43]. In the following subsections we revert to binary-distributed disorder, discussing the features of the phase diagram in some detail.

A. Incompressible phases

The boundaries of the incompressible Mott lobes have been derived in Ref. [25] based on a single-site mean-field effective theory. Reference [23] reports more quantitative results ensuing from strong-coupling perturbative expansions, which are further supported by density matrix renormalization group simulations. Reference [26] also provides results based on strong-coupling perturbative expansions, as well as on exact diagonalization of small 1D systems. Here we discuss site-dependent mean-field results and show that, unlike effective single-site mean-field theories, they do not depend on the impurity density p_0, as is expected.

We first of all observe that in the so-called "atomic limit" $t/U \to 0$ the ground state of Hamiltonian (1) is a product of on-site Fock states. That is, Eq. (5) applies exactly with $c_{j\nu} = \delta_{j\nu_j}$, where $\nu_j = \max\{0, \lceil(\mu - v_j)/U\rceil\}$ and the chemical potential μ is determined by the constraint on the total number $N = \Sigma_j \nu_j$. Recalling that the local potential v_j is Δ at $N_{\rm imp} = p_0 M$ randomly placed lattice sites and 0 at the remaining $M - N_{\rm imp}$ sites, it is easy to conclude that the total number of bosons is zero for $-\infty \leqslant \mu/U \leqslant 0$, and subsequently grows stepwise with increasing chemical potential. The staircase function is easily determined if $0 \leqslant \Delta/U \leqslant 1$. In this case the rises of the steps occur at $\mu_k(x) = kU + x$, with $k = 0, 1, \ldots, \infty$ and $x = 0, \Delta$. The height of the steps is $N = M(k+1) - N_{\rm imp}$ for $\mu_k(0) \leqslant \mu \leqslant \mu_k(\Delta)$ and $N = M(k+1)$ for $\mu_k(\Delta) \leqslant \mu \leqslant \mu_{k+1}(0)$. In the first case the wave function (5) is such that $|\psi_j\rangle = |k\rangle$ at the $N_{\rm imp}$ sites with $v_j = \Delta$, and $|\psi_j\rangle = |k+1\rangle$ at the remaining sites, where $|k\rangle = (a_j^\dagger)^k |\Omega\rangle/\sqrt{k!}$ is the local k-th Fock state. In the second case $|\psi_j\rangle = |k+1\rangle$ at every lattice site.

It is straightforward to check that these states diagonalize the mean-field Hamiltonian (6) subject to the self-consistency constraint (8) also for any $t > 0$, although they do not always represent the mean-field ground-state of the system. As it is illustrated in Sec. B, this is true only within the regions of the $\mu/U - t/U$ phase plane described by $0 \leqslant t/U \leqslant |\lambda_{\max}|^{-1}$, where $\lambda_{\max}$ is the maximal eigenvalue of the matrix

$$\Lambda = DA, \quad D_{m,m'} = \delta_{m,m'} \mathcal{B}^{-1}\left(\frac{\mu - v_m}{U}\right), \tag{19}$$

A is the adjacency matrix of the lattice, and the function $\mathcal{B}$ appearing in the diagonal matrix D is defined in Eq. (16). The numerical diagonalization of Λ at different values of μ shows that the above discussed plateaus extend over lobelike regions with alternatively noninteger and integer fillings.

Since in both cases $\alpha_j = 0$ we classify these phases as incompressible Mott insulators. As we have discussed above, the superfluid fraction expectedly vanishes. However, integer- and fractional-filling insulating phases are distinguished by the correlation with the underlying local potential. The former are homogeneous despite the presence of such a potential. The latter are clearly characterized by a disorder directly related to that in the location of the impurities described by the local potential v_j. We observe that these two incompressible phase are expected to exhibit different excitation spectra, which are relevant experimental quantities [5]. More to the point, the excitation spectrum of the integer-filling Mott phases will be characterized by three peaks at $U - \Delta$, U, and $U + \Delta$. As to the noninteger-filling lobes, the peaks are expected at Δ, U and, for fillings larger than 1, at $2U - \Delta$.

The data points in Fig. 1 have been obtained by evaluating the maximal eigenvalue of the matrix Λ as a function of the chemical potential for a 1D lattice comprising $M = 10^5$ sites. Black and white circles correspond to different impurity densities $N_{\rm imp} = 0.2M$ and $N_{\rm imp} = 0.6M$. Both data sets show a very good agreement with the analytic result in Eq. (18) and, as expected [23,26], exhibit no dependence on the impurity density $p_0 = N_{\rm imp}/M$. As briefly recalled in Appendix B, the same result can be equivalently obtained by studying the matrix $\Gamma = \sqrt{D} A \sqrt{D}$ which, unlike Λ, is symmetric, $\Gamma = \Gamma^t$.

We emphasize that mean-field results based on effective single-site results can be recovered by averaging the above matrices over disorder. We first of all observe that the disorder-averaged version of Λ results in the critical boundaries

$$\frac{t}{U} = \frac{1}{2d}\left[p_0 \mathcal{B}^{-1}\left(\frac{\mu - \Delta}{U}\right) + (1 - p_0)\mathcal{B}^{-1}\left(\frac{\mu}{U}\right)\right]^{-1}, \tag{20}$$

i.e., precisely the same result obtained by the so-called "simple man's" mean-field theory of Ref. [25]. Note that Eq. (20) is indeed a simplified result, in that it depends on the impurity density p_0, contrary to expectations [23,26]. We also observe that equivalent simplified approaches have been adopted in earlier papers [12,19], albeit with a different disorder distribution, and date back to the seminal work by Fisher *et al.* [1]. A perhaps more structured effective single-site theory is obtained from the disorder averaged version of the matrix Γ matrix defined above. Indeed the boundary of the $\alpha_j = 0$ phase ensuing from such matrix in the case of uniformly distributed disorder $p(v_j) = \Theta(v_j + \Delta/2)\Theta(\Delta/2 - v_j)$ is very similar to that provided by the stochastic mean-field theory described in Ref. [16]. However, it is quite clear that in the case of the binary distribution in Eq. (2) such boundary again depends on the impurity density p_0, just like in Eq. (20).

In the above general discussion we assume $0 < \Delta < U$. For $\Delta > U$ the arrangement of the first few lobes changes straightforwardly. For instance, for $U < \Delta < 2U$ the unitary-filling lobe disappears, the basis of the lobe at filling $1 - p_0$ extends in the whole interval $0 \leqslant \mu \leqslant U$ and the interval $U \leqslant \mu \leqslant \Delta$ provides the basis for a lobe with filling $2 - 2p_0$. Note that if $p_0 = 1/2$ this last lobe has unitary filling, although this results from averaging sites at filling 0 and 2. Hence the unitary-filling incompressible phase changes from homogeneous to disordered as Δ becomes larger than U. This was observed in an early work, where, however, the disordered, incompressible insulating phase is identified as a Bose-glass phase [24]. Clearly, the phase diagram of the homogeneous lattice is recovered for $\Delta = 0$, while the case $\Delta < 0$ can be

mapped on the repulsive case with the suitable number of impurities $\Delta \to |\Delta|$, $N_{\mathrm{imp}} \to M - N_{\mathrm{imp}}$.

B. Partially compressible phase, Bose glass

In order to discuss the situation in the partially compressible regions it proves convenient to introduce the notions of favorable and unfavorable sublattices for bosons added to the system, as determined by the competition by the local boson-boson interaction strength U and the local impurity potential $\Delta < U$. Clearly, in the absence of bosons the impurity-free sublattice $v_j = 0$ is energetically favorable. If some bosons are introduced in the system, they will prefer the impurity-free sites, as far as the local energy is concerned. However, at some fillings, the presence of bosons in the impurity-free sublattice could make the impurity sites more convenient energetically. Thus the favorable sublattice coincides with the impurity-free sublattice or with the impurity sublattice depending on the filling or, equivalently, on the chemical potential. Typically, the impurity sites are preferred in the partially uncompressible regions to the left of the integer filling uncompressible lobes (marked by Δ in Fig. 1), whereas the impurity-free sites are preferred in the remaining regions (marked by 0 in Fig. 1). We call "unfavorable" the sites of the lattice not belonging to the favorable sublattice.

The partial compressibility of the regions we are considering arises from the presence of arbitrarily large unfavorable regions behaving as homogeneous systems. Hence there are arbitrarily large sublattices hosting an uncompressible phase characterized by $\alpha_j = 0$. However, owing to the hopping term, not all of the unfavorable sites are characterized by vanishing order parameter. This allows for the formation of a cluster of $\alpha_j > 0$ sites spanning the entire lattice, and therefore capable of supporting a superfluid flow, even if the favorable sites do not percolate throughout the lattice. That is to say, the superfluidity is not related to the percolation of the favorable sublattice, but rather to the percolation of the sites where $\alpha_j > 0$. The latter is made possible by the quantum tunneling effect, which allows for the bridging of possibly disconnected clusters of favorable sites. We have studied this phenomenon at $\mu = \Delta = 0.5$, i.e., where the partially uncompressible regions of the phase diagram extend down to vanishing hopping amplitude. As it is shown in Fig. 2, both in 1D and 2D we observe a behavior of the form $f_s \propto (t/U)^L$, where L is the (integer) percolation length, i.e., the length of the longest "bridge" among those necessary to turn a disjoint impurity distribution into the shortest cluster spanning the whole lattice (see Fig. 3). Note that the same p_0 can give a different L due to finite-size fluctuations. This is especially clear on 1D system, where one expects $L = \infty$ in the thermodynamic limit, independent of p_0. However, once an L is determined by the actual finite-size realization of the disordered system, it dictates the behavior of f_s as discussed above and demonstrated in Fig. 2.

Now on one-dimensional lattices the percolation length corresponds to the size of the largest homogeneous cluster in the unfavorable lattice, which becomes arbitrarily large in the thermodynamic limit, independent of the impurity density. Hence in 1D the partially compressible phase is expected to be insulating for any finite impurity density as observed in Refs. [23,26].

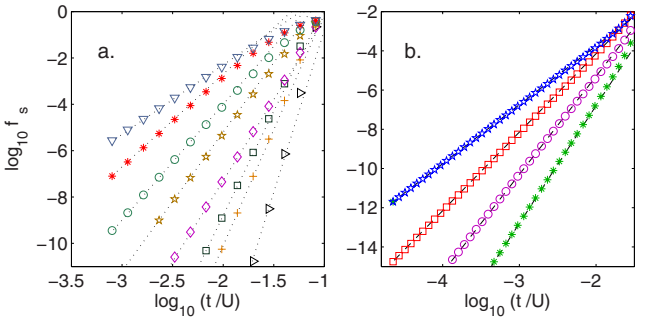

FIG. 2. (Color online) Power law decay of the superfluid fraction as a function of t/U. The left panel refers to a 1D lattice comprising $M = 400$ sites. The different data sets have been obtained by varying the impurity density between 0.4 and 0.7. The right panel corresponds to a 2D system, also comprising $M = 400$ sites, where the impurity density varies between 0.005 and 0.1. In every case the data sets are well described by a straight line having an integer slope which is found to coincide with the percolation length L (see Fig. 3). In the 1D case (left) we observe lengths from 3 to 14. In the 2D case $L = 3, 4, 5, 6$.

Conversely, on higher dimensional lattices the superfluid fraction is finite at any impurity density, although it can become extremely small. This is due to the fact that, unlike the one-dimensional case, L never diverges in the thermodynamic limit. This can be understood by observing that quantum tunneling introduces a long-range connectivity between the possibly disjoint clusters forming the favorable sublattice, which effectively increases the density of favorable sites. It is then clear that a sufficiently large hopping amplitude can bring the effective density of favorable sites above the (finite) percolation threshold, so that an effective spanning cluster is formed [44]. This concept is illustrated by the light gray regions in Fig. 3.

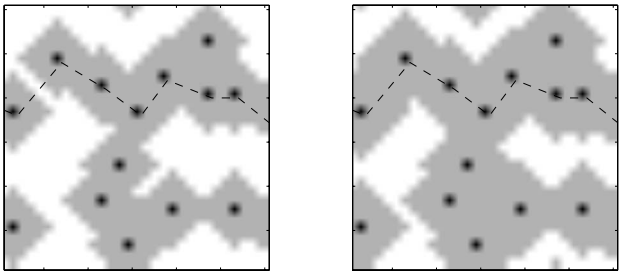

FIG. 3. A sketch illustrating the notion of percolation length. A 30 by 30 square lattice contains 14 favorable sites, signalled by the black squares. Due to their very low density they do not form a cluster spanning the lattice. The dashed line signals the shortest path allowing to "wade" through the lattice by stepping on favorable sites. The longest jump has to be taken between the first and the second favorable site from the left. The gray shading demonstrates the effective increase in the density of favorable sites caused by the long-range connectivity introduced by quantum tunneling. The range of such connectivity is 4 (left panel) or 5 (right panel) lattice constants. The shading in the right-most panel shows that the longest jump in the dashed path measures ten lattice constants. Hence $L = 10$ for this favorable sublattice.

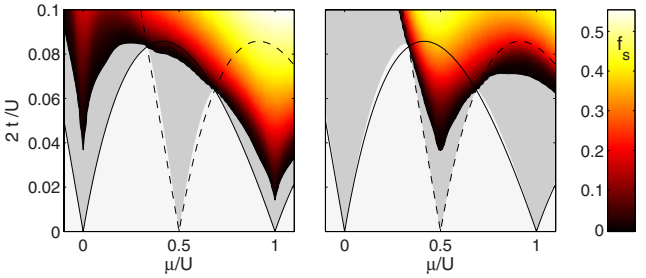

FIG. 4. (Color online) Phase diagram as determined from a numerical simulation on a 1D lattice comprising $M=961$ sites and containing $N_{\mathrm{imp}}=200$ (left) and $N_{\mathrm{imp}}=600$ (right) randomly located impurities. In both cases $\Delta=0.5U$, as in Fig. 1. The density plot represents the superfluid fraction as specified by the color bar. The uniform dark grey areas enclose the region where f_s is smaller than 1% of its largest value in the entire examined area. The uniform light grey areas are the fully incompressible Mott lobes determined as described in Sec. IV A. The solid and dashed black curves are the boundaries involved in Eq. (16). They are the same as in Fig. 1.

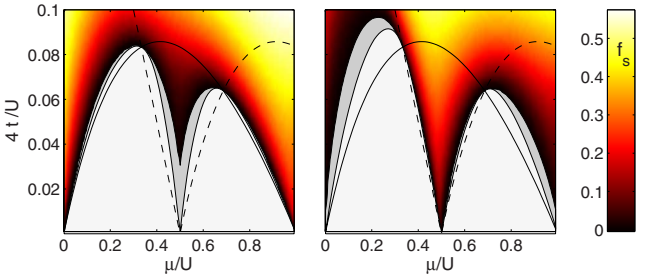

FIG. 5. (Color online) Phase diagram as determined from a numerical simulation on a 2D lattice comprising $M=31\times31=961$ sites and containing $N_{\mathrm{imp}}=200$ (left) and $N_{\mathrm{imp}}=600$ (right) randomly located impurities. In both cases $\Delta=0.5U$, as in Figs. 1 and 4.

C. Finite-size effects

The above discussion is valid in the thermodynamic limit. As we illustrate in the following, strong deviations from the expected behavior can be observed on finite-size lattices, even for fairly large sizes. In particular, on 1D systems a finite superfluid fraction can be observed in the partially compressible regions of the phase diagram. Conversely, on higher dimensional system, the expectedly finite superfluid fraction in the same regions may become so small that the phase can be considered insulating for any practical purpose. This agrees with the intuitive notion of a glass as an extremely viscous fluid.

These observations are applicable to the experimental realizations of the disordered Bose-Hubbard Hamiltonian (1)—whose size is necessarily finite—provided that the effects of the further trapping potential possibly involved in the experimental setup are negligible [45]. In order to demonstrate the relevance of these effects we have carried out numerical simulations for 1D and 2D lattices comprising $M=961$ sites. In both cases we have adopted periodic boundary conditions, and a constant velocity field parallel to a coordinate direction. The resulting phase diagrams, where we took into account that vanishingly small superfluid fractions can be considered zero, are shown in Figs. 4 and 5. The first thing to be noticed is that finite-size effects do not dramatically affect the boundaries of the fully incompressible Mott lobes, especially in one dimension. A slight dependence on the impurity density p_0 is observed, at variance with the thermodynamic limit result. In general, as is explained in Appendix B, the finite size lobes "enclose" those in the thermodynamic limit. Significant finite size effects are instead evident in the partially compressible phase. As we mention above, in the thermodynamic limit one expects this phase to be insulating in 1D, and superfluid for $d>1$. Actually, as it is clear from Figs. 4 and 5, these are the predominant characters of the partially compressible phases also on finite-size lattices. However, on 1D lattices significant portions of the partially compressible phase are superfluid. Conversely, on 2D lattices small partially compressible regions surrounding the Mott lobes exhibit exponentially small superfluid fractions, so that they can be considered virtually insulating. These deviations of the partially compressible phase from the expected behavior in the thermodynamic limit are strongly dependent on the impurity density p_0. In particular, for small impurity densities the partially compressible regions marked Δ in Fig. 1 tend to be more insulating than those marked 0. The converse occurs at large impurity densities. We emphasize that the favorable sublattice does not percolate at either of the chosen impurity densities. Hence, the fact that $f_s>0$ in the partially compressible phases must be attributed to quantum tunneling effects.

V. SUMMARY

In this paper we address the phase diagram of the Bose-Hubbard model describing ultracold bosonic atoms loaded in an optical lattice containing static random local impurities. These are fermionic atoms whose hopping amplitude has been quenched to extremely low values. We employ a site-dependent Gutzwiller scheme, analyzing both 1D and 2D lattices. On the one hand we show that this approach confirms that the phase diagram of the system does not depend on the density of impurities and can be easily derived from the phase boundary of the homogeneous case, at least with respect to the compressibility of the system. We show that the boundaries of the insulating fully incompressible region of the phase diagram are strictly related to the spectral radius of two (block) tridiagonal matrices. We discuss the expected modifications in the structure of the experimental excitation spectrum of the system occurring due to the presence of the noninteger-filling incompressible lobes appearing in the phase diagram in the presence of binary disorder. Also we provide exact formulas for the superfluid fraction and the fluxes induced by an infinitesimal velocity field, showing that these quantities ultimately depend on the mean-field order parameters alone. These formulas allow us to investigate the superfluid nature of the partially compressible regions appearing in the phase diagram of the system owing to the binary disorder. We discuss finite-size effects relevant to experimental realizations of the system under investigation, showing that they strongly depend on the impurity density

and mainly affect the boundaries of the partially compressible regions. We show that on one-dimensional system quantum percolation causes the appearance of superfluid domains within these regions. On the other hand, on higher dimensional lattice the in-principle superfluid partially compressible regions contain domains that can be considered virtually insulating, due to the extreme smallness of the superfluid fraction.

Last but not least, in the appendixes we provide the explicit derivation of the analytic results employed in the paper, whose validity is not limited to the case of binary distributed disorder. In particular, we discuss the relation the site-dependent Gutzwiller approach and effective single site mean-field theories.

ACKNOWLEDGMENTS

The authors wish to thank A. Mering for his extremely valuable comments and suggestions. The work of P.B. has been supported by the CNISM project "Quantum Phase Transitions, Nonlocal Quantum Correlations and Nonlinear Dynamics is Ultracold Lattice Boson Systems." The work of F.M. has been partially supported by the MIUR project "Cooperative Phenomena in Coherent Systems of Condensed Matter and their Realization in Atomic Chip Devices."

APPENDIX A: NORMAL MODES OF THE GUTZWILLER DYNAMICS

As we mention in Sec. III, a variational principle analogous to that described in Ref. [39] results in the set of dynamical equations for the expansion coefficients of the Gutzwiller state (5) [10,40]:

$$i\dot{c}_{j\nu} = \frac{U}{2}\nu(\nu-1)c_{j\nu} + v_j\nu c_{j\nu} - t(\gamma_j^*\sqrt{\nu+1}c_{j\nu+1} + \gamma_j\sqrt{\nu}c_{j\nu-1}), \tag{A1}$$

$$\gamma_j = \sum_h A_{jh}\alpha_h, \quad \alpha_h = \sum_{\nu=0}^{\infty}\sqrt{\nu+1}c_{j\nu}^* c_{j\nu+1}. \tag{A2}$$

It is straightforward to check that the norm of each on-site Gutzwiller factor, and the (average) total number of bosons in the system

$$\langle\psi_j|\psi_j\rangle = \sum_{\nu=0}^{\infty}|c_{j\nu}|^2, \quad N = \sum_j\sum_{\nu=0}^{\infty}\nu|c_{j\nu}|^2 \tag{A3}$$

are conserved by the dynamics.

The fixed-point condition $\dot{c}_{j\nu}=0$ for Eq. (A1) results in the set of equations

$$0 = \left[-\epsilon_j + \frac{U}{2}\nu(\nu-1) + (v_j-\mu)\right]\nu c_{j\nu} - t(\gamma_j^*\sqrt{\nu+1}c_{j\nu+1} + \gamma_j\sqrt{\nu}c_{j\nu-1}), \tag{A4}$$

where μ and $\{\epsilon_j\}$ are $M+1$ Lagrange multipliers ensuring that the total number of bosons and the norms of the Gutzwiller factors $|\psi_j\rangle$ equal the desired values.

But Eq. (A4) is nothing but the eigenvalue equation for the on-site mean-field Hamiltonian (7) projected onto the generic Fock state at site j, $|\nu\rangle=(a_j^\dagger)^\nu|\Omega\rangle/\sqrt{\nu!}$,

$$\langle\nu|\mathcal{H}_j - \epsilon_j|\psi_j\rangle = 0, \tag{A5}$$

where we recall that $a_h|\Omega\rangle=0$ for all h's. Note indeed that Eq. (A2), which must be considered part of Eq. (A1), is exactly equivalent to the self-consistency constraint specified by Eq. (8). By comparing Eqs. (A4) and (A1) we see that the solutions of the mean-field equations are normal modes of the Gutzwiller dynamics such that $c_{j\nu}(t)=e^{-it(\epsilon_j+\mu\nu)}c_{j\nu}(0)$. The fixed-point nature of these solutions becomes clear when one considers the relevant expectation values on Hermitian operators, corresponding to observable quantities. It is easy to verify that number-conserving Hermitian operators, such as, for instance, $a_k^\dagger a_h + a_h^\dagger a_k$, produce time-independent expectation values, whereas non-number-conserving Hermitian operators, such as $a_h^\dagger + a_h$, produce expectation values oscillating around 0. Note that the latter should be identically zero, since the original Hamiltonian (1)—unlike its mean-field counterpart—commutes with the total number of bosons. This result is recovered after time averaging the expectation values.

Note finally that $E=\langle\Psi|H|\Psi\rangle=\langle\Psi|\mathcal{H}+\mu N|\Psi\rangle$, and that $\mathcal{H}$ can be obtained from $H-\mu N$ by assuming that $a_j^\dagger a_k = a_j^\dagger\alpha_k + \alpha_j^* a_k - \alpha_j^*\alpha_k$ for $j\neq k$, where $\alpha_j=\langle\Psi|a_j|\Psi\rangle=\langle\psi_j|a_j|\psi_j\rangle$ [37]. As is shown in Refs. [39,46] the time—dependent variational principle approach based on Glauber's and SU(M) coherent states instead of those in Eq. (5) gives the discretized Gross-Pitaevskii equations for the Bose-Hubbard model (1). Interestingly, the Gutzwiller mean-field states in Eq. in Eq. (5) reduce to Glauber's coherent states for $U\to 0$, as it is clear from the form of the mean-field Hamiltonian (6) [40].

APPENDIX B: MOTT PHASE BOUNDARY

In this appendix we show that the critical boundary of the (mean-field) Mott phase, ($\alpha_j=0$ for every j) is the inverse of the maximal eigenvalue of the matrix Λ defined in Eq. (19). Since $\alpha_j=0$ everywhere, we also have $\gamma_j=0$ at every site, according to Eq. (8). Hence the mean-field Hamiltonian (6) is the sum of the on-site Hamiltonians in Eq. (7) and the ground state (5) is bound to be a product of local Fock states

$$|\psi\rangle = |\nu\rangle = \frac{(a^\dagger)^\nu}{\nu!}|0\rangle, \quad \nu = \left\lceil\frac{\mu-v}{U}\right\rceil. \tag{B1}$$

The relevant on-site energy is

$$\epsilon_\nu = \frac{U}{2}\nu(\nu-1) + (v-\mu)\nu. \tag{B2}$$

Hence $\langle\Psi|a_j|\Psi\rangle=0$ at every site, and the self-consistency constraint (8) is satisfied. Note that Eq. (8) defines a map, since any set of (possibly nonzero) α_j determines a set of local ground states $|\psi_j\rangle$ via Hamiltonian (6), which in turn determines a new set of α_j. This is by definition a fixed point of the map when it coincides with the original set, which is

exactly what happens for the configuration under examination, $\alpha_j=0$, for any choice of the Hamiltonian parameters. However, the stability of such a "trivial fixed point" does depend on the Hamiltonian parameters. Specifically, the fixed point is stable only if the maximal eigenvalue of the linearized version of the map is smaller than 1. In order to linearize the map we assume that $|\alpha_j| \ll 1$, which yields $|\gamma_j| \ll 1$ and treat the (mean-field) kinetic term in Hamiltonian (6) as perturbative. Dropping for a while the site label we get, up to the first perturbative order,

$$|\psi\rangle = |\psi^{(0)}\rangle + |\psi^{(1)}\rangle, \tag{B3}$$

$$|\psi^{(1)}\rangle = -t \sum_{\nu' \neq \nu} \frac{\langle \nu' | \gamma a^\dagger + \gamma^* a | \nu \rangle}{\epsilon_\nu - \epsilon_{\nu'}} |\nu'\rangle, \tag{B4}$$

$$|\psi\rangle = |\nu\rangle - \frac{t\gamma\sqrt{\nu+1}}{\epsilon_\nu - \epsilon_{\nu+1}} |\nu+1\rangle - \frac{t\gamma^*\sqrt{\nu}}{\epsilon_\nu - \epsilon_{\nu-1}} |\nu-1\rangle, \tag{B5}$$

where $|\nu\rangle$, ν, and ϵ_ν are defined in Eqs. (B1) and (B2). Hence

$$\begin{aligned} \langle \psi | a | \psi \rangle &= -t\gamma \left(\frac{\nu+1}{\epsilon_\nu - \epsilon_{\nu+1}} + \frac{\nu}{\epsilon_\nu - \epsilon_{\nu-1}} \right) \\ &= -\gamma \frac{t(U+\mu-v)}{(\nu U + v - \mu)(\nu U - U + v - \mu)}. \end{aligned} \tag{B6}$$

Restoring the site label, recalling the definition of γ_m [Eq. (8)], ν [Eq. (B1)], and $\mathcal{B}$ [Eq. (16)] one gets

$$\begin{aligned} \langle a_m \rangle &= \frac{t}{U} \mathcal{B}^{-1}\left(\frac{\mu - v_m}{U} \right) \sum_{m'} A_{mm'} \langle a_{m'} \rangle, \\ &= \frac{t}{U} \sum_{m'} \Lambda_{mm'} \langle a_{m'} \rangle, \end{aligned} \tag{B7}$$

where Λ is the same as in Eq. (19). Recalling the criteria for the stability of linear maps, the fixed point $\langle a_m \rangle = 0$ (equivalent to $\gamma_m = 0$) is stable whenever

$$\frac{t}{U} \leqslant \frac{1}{|\lambda_{\max}|}, \tag{B8}$$

where $\lambda_{\max}$ is the eigenvalue of Λ with the largest magnitude.

We note that despite $\Lambda^t \neq \Lambda$, the spectrum of this matrix is real. This can be explained by observing that the eigenvalue problem $\underline{\Lambda}\mathbf{x} = \lambda \mathbf{x}$ is equivalent to $\Gamma \mathbf{y} = \lambda \mathbf{y}$, where $y_j = D^{-1}_{j,j} x_j$ and $\Gamma = \sqrt{D} A \sqrt{D} = \Gamma^t$. Recalling that the maximal eigenvalue of a matrix coincides with its two-norm one can derive a lower bound for the critical hopping to interaction ratio. Indeed

$$\frac{1}{|\lambda_{\max}|} = \frac{1}{\|\Lambda\|_2} \geqslant \frac{1}{\|D\|_2 \|A\|_2} = \left[2d \min_{\{v_j\}} \mathcal{B}^{-1}\left(\frac{\mu - v_j}{U} \right) \right]^{-1}. \tag{B9}$$

Note that in the case of binary distributed disorder Eq. (B9) coincides with Eq. (18). Hence, the finite-size lobes always enclose their thermodynamic counterparts.

It is interesting to observe that the above approach naturally suggests two disorder-averaged effective theories. Indeed, one could trade the matrix elements of Λ or Γ with their averages over disorder. This would give

$$\frac{t}{U} < \frac{1}{2d} \left[\int dv p(v) \mathcal{B}^{-1}\left(\frac{\mu - v}{U} \right) \right]^{-1} \tag{B10}$$

for Λ and

$$\frac{t}{U} < \frac{1}{2d} \left[\int dv p(v) \mathcal{B}^{-1/2}\left(\frac{\mu - v}{U} \right) \right]^{-2} \tag{B11}$$

for Γ.

As mentioned in Ref. [13], Eq. (B10) gives the zero-temperature (analytical) phase diagram derived in Refs. [1,12,19] in the case of v uniformly distributed in $[-\Delta, \Delta]$. Interestingly, Eq. (B11) gives a different result, very similar to that obtained by the stochastic mean-field theory recently described in Ref. [16].

The integrations in Eqs. (B10) and (B11) can be easily carried out analytically in the case of a binary distributed disorder Eq. (2). In particular, it is quite straightforward to show that Eq. (B10) is equivalent to Eq. (20), which does not exhibit the expected independence on the impurity density $p_0 = N_{\text{imp}}/M$ in the thermodynamic limit, as discussed in Sec. IV. The same problem affects the boundary derived from Eq. (B11). These results seem to suggest that—at least in the case of binary disorder—effective single-site mean-field theories are not able to capture the thermodynamic limit.

APPENDIX C: SUPERFLUID FRACTION AND MEAN-FIELD APPROACH

In this section we derive the analytic expression for the phases ϕ_i introduced in Sec. III for the mean field study of the currents present in the system. Also, we obtain the analytic mean-field expression (11) for the superfluid fraction (3).

We first of all observe that expanding the θ-dependent terms in Eq. (1) one finds that even and odd contributions are purely real and imaginary, respectively [34]. As a result, this is true also of the ground-state perturbative expansion, while only even terms contribute to the ground-state energy.

In the Gutzwiller approximation, this implies that each factor of the perturbative expansion in Eq. (5) has the same alternating form: the even contributions are real and the odd contributions are imaginary. Hence, the same property holds also for the mean-field parameters α_m defined in Eq. (8).

Therefore, at first order in θ we can write

$$\alpha_j = \alpha_j^0 \exp(i\theta\phi_j), \tag{C1}$$

where $\alpha_j^0 = \langle \psi_j^0 | a_j | \psi_j^0 \rangle$ is the local mean-field parameter for $\theta = 0$, and $\phi_j \in \mathbb{R}$. Plugging the last result in Hamiltonian (7) in and keeping only first-order contributions one gets

$$\mathcal{H}_j = \frac{U}{2}(n_j - 1)n_j + (v_j - \mu)n_j - t a_j^\dagger r_j \exp(i\vartheta_j) + \text{c.c.}, \tag{C2}$$

where we denote

$$\vartheta_j = \theta \frac{\sum_i A_{ji}\alpha_i^0(B_{ji}+\phi_i)}{\sum_i A_{ji}\alpha_i^0}, \quad r_j = \sum_i A_{ji}\alpha_i^0. \tag{C3}$$

Let us define $\tilde{a}_j = a_j \exp(-i\vartheta_j)$. The new creation and destructions operators $\tilde{a}_j^\dagger$ and $\tilde{a}_j$ satisfy the same algebra of $a_j^\dagger$ and a_j and moreover $n_j = \tilde{a}_j^\dagger \tilde{a}_j$. By introducing these new operators the eigenvalue and the self-consistency equations become

$$E_j|\psi_j\rangle = \left[\frac{U}{2}(n_j-1)n_j + (v_j-\mu)n_j - t(\tilde{a}_j^+ + \tilde{a}_i)\sum_i A_{ji}\alpha_j^0\right]|\psi_j\rangle, \tag{C4}$$

$$\exp(i\vartheta_j)\langle\psi_j|\tilde{a}_j|\psi_j\rangle = \alpha_j^0 \exp(i\theta\phi_j). \tag{C5}$$

The solutions to Eqs. (C4) and (C5) can be directly obtained from the solutions of order 0 in θ. In particular if $|\psi_j^0\rangle = \Sigma_n c_{j,n}(a_j^+)^n|0\rangle$ is the on site wave function for $\theta=0$, to the first order in θ the on site wave functions are

$$|\tilde{\psi}_j^0\rangle = \sum_n c_{j,n}(\tilde{a}_j^+)^n|0\rangle = \sum_n c_{j,n}e^{-in\vartheta_j}(a_j^+)^n|0\rangle \tag{C6}$$

with $\vartheta_j = \theta\phi_j$. Moreover, as expected, there are no first-order contributions to the energy. Equation $\vartheta_j = \theta\phi_j$ entails that

$$\sum_i \left(\delta_{ji}\sum_k A_{jk}\alpha_k^0 - A_{ji}\alpha_i^0\right)\phi_i = \sum_i B_{ji}\alpha_i^0. \tag{C7}$$

Equations (C7) provide an expression for the phases ϕ_i, which can be plugged into Eq. (13), to obtain the currents to the first order in θ.

Let us consider the second order perturbation in θ. The contribution to the parameters α_j can be written as $\alpha_j = (\alpha_j^0 + \theta^2\xi_j)\exp(i\theta\phi_j)$. Within such an approximation the on site Hamiltonian is

$$\mathcal{H}_j = 1/2(n_j-1)n_j + (v_j-\mu)n_j - ta_j^+ r_j' \exp(i\theta\phi_j) + \text{c.c.} \tag{C8}$$

with

$$r_j' = \sum_i A_{ji}\alpha_i^0 + \theta^2\left(\sum_i A_{ji}\xi_i - \frac{1}{2}\sum_i A_{ji}\alpha_i^0(B_{ji}+\phi_i-\phi_j)^2\right). \tag{C9}$$

Equation (C9) has been obtained by expanding in θ and exploiting expression (C7). Therefore we have to solve the self consistency equations

$$\mathcal{H}_j^0 + \theta^2\mathcal{V}_j^0|\psi_j\rangle = E_j|\psi_j\rangle \tag{C10}$$

and

$$\langle\psi_j|\tilde{a}_j|\psi_j\rangle = (\alpha_j^0 + \theta^2\xi_j), \tag{C11}$$

where

$$\mathcal{H}_j^0 = 1/2(n_j-1)n_j + (v_j-\mu)n_j - t(\tilde{a}_j^+ + \tilde{a}_j)\sum_i A_{ji}\alpha_j^0,$$

$$\mathcal{V}_j = -t(\tilde{a}_j^+ + \tilde{a}_j)\left(\sum_i A_{ji}\xi_i - \frac{1}{2}\sum_i A_{ji}\alpha_i^0(B_{ji}+\phi_i-\phi_j)^2\right). \tag{C12}$$

Equations (C10) and (C11) are solved by a first order pertubation theory in θ^2. In particular denoting $|\psi_j\rangle = |\tilde{\psi}_j^0\rangle + \theta^2|\tilde{\psi}_j^2\rangle$ and $E_j = E_j^0 + \theta^2 E_j^2$ [with $|\tilde{\psi}_j^0\rangle$ given by Eq. (C6) and E_i^0 eigenvalue of the solution for $\theta=0$], we have

$$E_j^2 = \langle\tilde{\psi}_j^0|V_j|\tilde{\psi}_j^0\rangle, \tag{C13}$$

$$|\tilde{\psi}_j^2\rangle = -(H_J^0 - E_j^0)^{-1}V_j|\tilde{\psi}_j^0\rangle, \tag{C14}$$

and

$$\langle\tilde{\psi}_j^0|\tilde{a}_j + \tilde{a}_j^+|\tilde{\psi}_j^2\rangle = \xi_j. \tag{C15}$$

inserting Eq. (C14) into (C15) we obtain

$$\sum_i (A_{ji}X_j - \delta_{ij})\xi_i = \frac{X_j}{2}\sum_i A_{ji}\alpha_i^0(B_{ji}+\phi_i-\phi_j)^2 \tag{C16}$$

with $X_j = t\langle\tilde{\psi}_j^0|(\tilde{a}_j+\tilde{a}_j^+)(H_J^0-E_j^0)^{-1}(\tilde{a}_j+\tilde{a}_j^+)|\tilde{\psi}_j^0\rangle$. The quantities ξ_j are obtained from Eq. (C16) and E_j^2 is

$$E_j^2 = -2t\alpha_j^0\left(\sum_i A_{ji}\xi_i - \frac{1}{2}\sum_i A_{ji}\alpha_i^0(B_{ji}+\phi_i-\phi_j)^2\right). \tag{C17}$$

We recall that the mean field Hamiltonian (6) is composed by the sum of the on site terms $\mathcal{H}_i$ and of a diagonal term, which has been so far neglected, since it does not provide any contribution to the wave functions, and hence to the relevant expectation values. However, such term is not negligible in the evaluation of the system energy. In particular, it provides a contribution of $\Sigma_j E_j^d$ with $E_j^d = \alpha_j^* t/2\Sigma_i A_{ji}\alpha_i \exp(i\theta B_{ji}) + \text{c.c.}$ For small θ we get $E_j^d = E_j^{d0} + \theta^2 E_j^{d2}$ with

$$E_j^{d2} = t\alpha_j^0\left(\sum_i A_{ij}\xi_i - \frac{1}{2}\sum_i A_{ji}\alpha_i^0(B_{ji}+\phi_i-\phi_j)^2\right) + t\xi_j\sum_i A_{ji}\alpha_i^0 \tag{C18}$$

from definition (3) it is clear that

$$f_s = \frac{1}{tN}\sum_j E_j^2 + E_j^{d2} = \frac{\sum_{i,j} A_{ij}\alpha_i^0\alpha_j^0(B_{ji}+\phi_i-\phi_j)^2}{2N}. \tag{C19}$$

It is interesting to observe that on 1D systems there is no need to evaluate the phases ϕ_j, the superfluid fraction being determined by the α_j^0 alone. This can be proved by observing that on a 1D lattice the current in Eq. (13) is bound to have the same value across any couple of neighboring sites j and $j+1$. Recalling that $A_{ij} = \delta_{i,j+1} + \delta_{i,j-1}$ and $B_{ij} = \delta_{i,j+1} - \delta_{i,j-1}$, one gets $\mathcal{J}_{j,j+1} = -\mathcal{J}_{j+1,j} = \mathcal{J} = -2\theta t\alpha_j^0\alpha_{j+1}^0[\phi_j - \phi_{j+1} - 1]$. This yields

$$\sum_{j=1}^{M} \frac{1}{\alpha_j^0 \alpha_{j+1}^0} = \frac{2Mt\theta}{\mathcal{J}} \tag{C20}$$

and

$$\phi_j - \phi_{j+1} - 1 = -\frac{\mathcal{J}}{2\theta t \alpha_j^0 \alpha_{j+1}^0} = -\frac{M}{\alpha_j^0 \alpha_{j+1}^0} \left(\sum_{\ell=1}^{M} \frac{1}{\alpha_\ell^0 \alpha_{\ell+1}^0} \right)^{-1}. \tag{C21}$$

Plugging this result into Eq. (C19) gives

$$f_s = \frac{M^2}{N} \left(\sum_{j=1}^{M} \frac{1}{\alpha_j^0 \alpha_{j+1}^0} \right)^{-1} = \frac{\mathcal{J}}{2t\theta N/M}. \tag{C22}$$

We conclude by observing that the very same derivation of Eq. (C19) can be carried out in the case of discrete Gross-Pitaevskii equations, which, as described in Appendix A, ensue from assuming that the states in Eq. (5) are Glauber's or SU(M) coherent states. The resulting equations have exactly the same form as Eqs. (C7) and (C19), where the mean-field order parameter α_j is substituted by the corresponding coherent-state label z_j.

[1] M. P. A. Fisher, P. B. Weichman, G. Grinstein, and D. S. Fisher, Phys. Rev. B **40**, 546 (1989).

[2] M. Greiner, O. Mandel, T. Esslinger, T. W. Hansch, and I. Bloch, Nature (London) **415**, 39 (2002).

[3] L. Fallani, C. Fort, and M. Inguscio, in *Advances in Atomic, Molecular, and Optical Physics*, edited by C. L. E. Arimondo and P. Berman (Academic Press, New York, 2008).

[4] J. E. Lye, L. Fallani, M. Modugno, D. S. Wiersma, C. Fort, and M. Inguscio, Phys. Rev. Lett. **95**, 070401 (2005); T. Schulte, S. Drenkelforth, J. Kruse, W. Ertmer, J. Arlt, K. Sacha, J. Zakrzewski, and M. Lewenstein, *ibid.* **95**, 170411 (2005); D. Clement, A. F. Varon, M. Hugbart, J. A. Retter, P. Bouyer, L. Sanchez-Palencia, D. M. Gangardt, G. V. Shlyapnikov, and A. Aspect, *ibid.* **95**, 170409 (2005).

[5] L. Fallani, J. E. Lye, V. Guarrera, C. Fort, and M. Inguscio, Phys. Rev. Lett. **98**, 130404 (2007).

[6] S. Ospelkaus, C. Ospelkaus, O. Wille, M. Succo, P. Ernst, K. Sengstock, and K. Bongs, Phys. Rev. Lett. **96**, 180403 (2006).

[7] M. Wallin, E. S. Sörensen, S. M. Girvin, and A. P. Young, Phys. Rev. B **49**, 12115 (1994); B. V. Svistunov, *ibid.* **54**, 16131 (1996); M. B. Hastings, *ibid.* **64**, 024517 (2001); R. Graham and A. Pelster, e-print arXiv:cond-mat/0508306.

[8] R. T. Scalettar, G. G. Batrouni, and G. T. Zimanyi, Phys. Rev. Lett. **66**, 3144 (1991); W. Krauth, N. Trivedi, and D. Ceperley, *ibid.* **67**, 2307 (1991); G. G. Batrouni and R. T. Scalettar, Phys. Rev. B **46**, 9051 (1992); J. Kisker and H. Rieger, *ibid.* **55**, R11981 (1997); P. Hitchcock and E. S. Sorensen, *ibid.* **73**, 174523 (2006); J.-W. Lee and M.-C. Cha, *ibid.* **72**, 212515 (2005); H. Gimperlein, S. Wessel, J. Schmiedmayer, and L. Santos, Phys. Rev. Lett. **95**, 170401 (2005).

[9] T. Roscilde, Phys. Rev. A **77**, 063605 (2008).

[10] K. Sheshadri, H. R. Krishnamurthy, R. Pandit, and T. V. Ramakrishnan, Phys. Rev. Lett. **75**, 4075 (1995).

[11] B. Damski, J. Zakrzewski, L. Santos, P. Zoller, and M. Lewenstein, Phys. Rev. Lett. **91**, 080403 (2003).

[12] K. V. Krutitsky, A. Pelster, and R. Graham, New J. Phys. **8**, 187 (2006).

[13] P. Buonsante, V. Penna, A. Vezzani, and P. B. Blakie, Phys. Rev. A **76**, 011602(R) (2007).

[14] P. Buonsante, F. Massel, V. Penna, and A. Vezzani, Laser Phys. **17**, 538 (2007).

[15] P. Buonsante, F. Massel, V. Penna, and A. Vezzani, J. Phys. B **40**, F265 (2007).

[16] U. Bissbort and W. Hofstetter, e-print arXiv:0804.0007.

[17] K. G. Singh and D. S. Rokhsar, Phys. Rev. B **49**, 9013 (1994); R. V. Pai, R. Pandit, H. R. Krishnamurthy, and S. Ramasesha, Phys. Rev. Lett. **76**, 2937 (1996); S. Rapsch, U. Schollwöck, and W. Zwerger, Europhys. Lett. **46**, 559 (1999).

[18] G. Roux, T. Barthel, I. P. McCulloch, C. Kollath, U. Schollwöck, and T. Giamarchi, Phys. Rev. A **78**, 023628 (2008).

[19] J. K. Freericks and H. Monien, Phys. Rev. B **53**, 2691 (1996).

[20] A. M. Rey, I. I. Satija, and C. W. Clark, Phys. Rev. A **73**, 063610 (2006).

[21] R. Roth, Phys. Rev. A **66**, 013614 (2002); M. Cramer, J. Eisert, and F. Illuminati, Phys. Rev. Lett. **93**, 190405 (2004); A. Albus, F. Illuminati, and J. Eisert, Phys. Rev. A **68**, 023606 (2003); A. Sanpera, A. Kantian, L. Sanchez-Palencia, J. Zakrzewski, and M. Lewenstein, Phys. Rev. Lett. **93**, 040401 (2004); K. Sengupta, N. Dupuis, and P. Majumdar, Phys. Rev. A **75**, 063625 (2007).

[22] U. Gavish and Y. Castin, Phys. Rev. Lett. **95**, 020401 (2005).

[23] A. Mering and M. Fleischhauer, Phys. Rev. A **77**, 023601 (2008).

[24] R. Allub, Solid State Commun. **99**, 955 (1996).

[25] H. Fehrmann, M. A. Baranov, B. Damski, M. Lewenstein, and L. Santos, Opt. Commun. **243**, 23 (2004).

[26] K. V. Krutitsky, M. Thorwart, R. Egger, and R. Graham, Phys. Rev. A **77**, 053609 (2008).

[27] G. Refael and E. Demler, Phys. Rev. B **77**, 144511 (2008).

[28] F. Gerbier, A. Widera, S. Fölling, O. Mandel, T. Gericke, and I. Bloch, Phys. Rev. A **72**, 053606 (2005).

[29] We are interested in the phase diagram of Hamiltonian (1), which is rigorously defined in the thermodynamic limit. Hence we make the standard assumption that the system is engineered so that effects of the harmonic trapping potential typical of experiments can be safely neglected in the bulk of the lattice. In Sec. IV C we take into account the fact that the number of sites where this assumption applies is finite.

[30] B. Horstmann, J. I. Cirac, and T. Roscilde, Phys. Rev. A **76**, 043625 (2007).

[31] C. Wu, H.-D. Chen, J.-P. Hu, and S.-C. Zhang, Phys. Rev. A **69**, 043609 (2004).

[32] R. Bhat, L. D. Carr, and M. J. Holland, Phys. Rev. Lett. **96**, 060405 (2006).

[33] B. S. Shastry and B. Sutherland, Phys. Rev. Lett. **65**, 243 (1990).

[34] R. Roth and K. Burnett, Phys. Rev. A **67**, 031602(R) (2003).
[35] A. M. Rey, K. Burnett, R. Roth, M. Edwards, C. J. Williams, and C. W. Clark, J. Phys. B **36**, 825 (2003).
[36] W. Krauth, M. Caffarel, and J.-P. Bouchaud, Phys. Rev. B **45**, 3137 (1992).
[37] K. Sheshadri, H. R. Krishnamurthy, R. Pandit, and T. V. Ramakrishnan, Europhys. Lett. **22**, 257 (1993).
[38] D. Jaksch, C. Bruder, J. I. Cirac, C. W. Gardiner, and P. Zoller, Phys. Rev. Lett. **81**, 3108 (1998); J. Zakrzewski, Phys. Rev. A **71**, 043601 (2005); X. Lu and Y. Yu, *ibid.* **74**, 063615 (2006); M. Snoek and W. Hofstetter, *ibid.* **76**, 051603(R) (2007).
[39] L. Amico and V. Penna, Phys. Rev. Lett. **80**, 2189 (1998).
[40] D. Jaksch, V. Venturi, J. I. Cirac, C. J. Williams, and P. Zoller, Phys. Rev. Lett. **89**, 040402 (2002).
[41] O. Penrose and L. Onsager, Phys. Rev. **104**, 576 (1956).
[42] P. Louis and M. Tsubota, J. Low Temp. Phys. **148**, 351 (2007).
[43] P. Buonsante, V. Penna, and A. Vezzani, Phys. Rev. A **70**, 061603(R) (2004).
[44] M. Gouker and F. Family, Phys. Rev. B **28**, 1449 (1983); M. B. Isichenko, Rev. Mod. Phys. **64**, 961 (1992).
[45] We observe that a periodic 1D optical lattice with no harmonic potential could be realized as described in L. Amico, A. Osterloh, and F. Cataliotti, Phys. Rev. Lett. **95**, 063201 (2005).
[46] P. Buonsante, V. Penna, and A. Vezzani, Phys. Rev. A **72**, 043620 (2005); P. Buonsante and V. Penna, J. Phys. A **41**, 175301 (2008).